Symbol Timing and Carrier Frequency Recovery Based on Entropy Minimization

XIAO LIU, (Student Member, IEEE), AND JEAN-FRANÇOIS BOUSQUET, (Member, IEEE)

Department of Electrical and Computer Engineering, Dalhousie University, Halifax, NS B3J 1Z1, Canada

Corresponding author: Jean-François Bousquet (jbousquet@dal.ca)

ABSTRACT This paper presents a new entropy minimization criterion for both symbol timing and carrier frequency recovery for wireless receivers. Synchronization is achieved by minimizing the entropy estimated from the eye diagram and the constellation diagram. Key implementation details are addressed toward the realization of entropy-based synchronization algorithms. In addition, the performance is evaluated in controlled conditions. It is shown that, as an alternative to the maximum likelihood criterion, entropy minimization has great potential and offers certain advantages for synchronization in wireless communication, particularly for pulse shaping filters with small excess bandwidth, as well as in multipath fading channels.

INDEX TERMS Entropy minimization, symbol timing, carrier recovery, synchronization, multipath.

I. INTRODUCTION

In coherent wireless communications systems, synchronization is a key operation at the receiver; it is usually realized between the matched filter and the equalizer. The two main functions of the synchronizer are symbol timing and carrier recovery. The purpose of symbol timing recovery is to recover the symbol clock from the modulated waveform, so that it can down-sample the waveform with the correct symbol timing offset (STO). Hence, at the output of a matched filter, a signal that is sampled at the ideal instant can have maximum signal to noise ratio (SNR) and no intersymbol interference (ISI) [1]. Also, to recover the information embedded in the phase modulation in coherent communication systems, the down converter must have exactly the same frequency as the carrier of the signal. However, in practice, the local oscillator frequency deviates from the input signal's carrier frequency. As such, the carrier frequency offset (CFO) has to be compensated. Moreover, in some applications, such as underwater acoustic communications, the channel may constantly change due to the time-variant environment or Doppler effect. Therefore a continuous and fast estimation and compensation of the STO and CFO is essential to maintain the link reliability.

Various synchronization algorithms have been described in the literature. While data-aided (DA) synchronization offers a superior performance, in this work, non-data-aided (NDA) schemes are approached to maintain a high spectral efficiency. A feedforward timing correction architecture is described for fast convergence rate.

Most synchronization algorithms follow the maximum likelihood (ML) criterion or its approximation. For example, the Oerder and Meyr (O&M) algorithm [2] is a square-law nonlinearity (SLN) estimator exploiting the cyclostationary properties of the modulated signal, and is one of the most commonly used NDA feedforward STO estimator. It has been proven that this algorithm and its variants [3] can be asymptotically interpreted as an ML estimator [4], [5]. For feedback configurations, the NDA Gardner timing error detector and its DA counterpart, the zero-crossing detector can also be derived from the ML criterion [1]. The NDA feedforward CFO estimator proposed in [6] employs the fourth-order cyclostationary property, and still follows the ML criterion. Also, various DA feedforward CFO estimators attempt to maximize the inner product between the training sequence and the data samples. All these CFO estimators can be treated as generalized ML estimators [1].

The primary contribution of this paper consists in the definition of a unified synchronization criterion, relying on entropy minimization (EM) as an alternative to the ML criterion. Specifically, the entropy of the eye diagram is evaluated for symbol timing recovery, and the entropy of the constellation diagram is measured for carrier frequency recovery. For both applications, the synchronization parameter that leads to a minimum entropy value is considered to be optimum. A similar concept, the minimum error entropy which is an important and highly effective optimization criterion in information theoretic learning can be found in [7]. Note that it

has been shown in [8] that the CFO of phase-shift keying (PSK) and quadrature amplitude modulation (QAM) modulated signals can be recovered by minimizing the entropy of the instantaneous phase probability density function (PDF), and the phase entropy is obtained by linear search with high computational complexity. In comparison, in the proposed work, a more generic entropy criterion is employed, where both the phase and amplitude components are considered. This concept has been briefly introduced in our previous work [9]. However, to the best of the authors' knowledge, this is the first work that provides a non-ML, unified criterion for both symbol timing and carrier recovery and that also includes an extensive conceptual analysis.

For demonstration purposes, a custom estimation algorithm is provided to evaluate the entropy of the signal eye diagram and constellation. Many practical issues can be encountered when implementing EM based synchronization algorithms. These issues include undesired local minima, insufficient oversampling rate and the vanishing of the gradient. The next contribution of this work is a practical implementation that addresses these issues.

The performance of the proposed symbol timing and carrier frequency recovery criterion is also evaluated in controlled conditions. The effects of various channel impairments, including noise and multipath, are analyzed on the system performance. The EM based algorithms are found to have improved performance when the pulse shaping filter has a small excess bandwidth, so that it allows better spectral efficiency. It is also demonstrated that the EM criterion provides a higher SNR than the ML criterion for timing recovery in multipath channels.

This paper is organized as follows. In Section II, an entropy minimization criterion for synchronization is introduced. A customized entropy estimation algorithm, and its implementation issues are discussed in Section III. In Section IV, the performance of the algorithm is evaluated in controlled conditions. Finally, conclusions are drawn in Section V.

II. ENTROPY MINIMIZATION BASED SYNCHRONIZATION
In this section the entropy minimization criterion is presented. Specifically, the signal model adopted in this paper is presented in Section II-A. The standard ML criterion is briefly introduced in comparison to the EM criterion in Section II-B. Then, the application of the EM criterion to symbol timing using the eye diagram entropy is explained in Section II-C, while the constellation diagram entropy used for carrier frequency recovery is explained in Section II-D.

A. SIGNAL MODEL
In this work, it is assumed that the signal is transmitted using coherent modulation schemes with an alphabet size of M, where M is a power of two. In the following discussion, quadrature phase shift keying (QPSK) modulation is used to validate the performance, but the application is not limited to low order modulation schemes. In fact, the discussion can be easily extended to other PSK or QAM modulations.

The received binary information follows an independent identical distribution (i.i.d.). The modulated data are pulse shaped to limit the bandwidth occupancy. A standard pulse shaping filter is used at the transmitter, which is designed under the Nyquist criterion, such that there is no ISI at the ideal sampling instants.

At the receiver, the over-sampled passband signal goes through a down converter and a matched filter first. Then, a timing recovery is applied, and it is followed by a carrier frequency recovery. Such a design is based on the idea that the decimated samples are sufficient for the CFO estimation, and the estimation has less computational burden because it operates at a reduced rate.

At baseband, the i-th data sample x_i after timing and carrier frequency recovery can be expressed as [10]

$$x_i[\tau, f_\Delta] = y(iT + \tau, f_\Delta)e^{-j2\pi f_\Delta iT}, \tag{1}$$

where y is the output of the matched filter, τ and f_Δ are the STO and the CFO respectively, and T is the symbol period. To estimate the STO and CFO, the EM criterion will be presented in Section II-C and Section II-D respectively.

B. MAXIMUM LIKELIHOOD VERSUS ENTROPY MINIMIZATION
The estimation of the STO and CFO can be considered to be an optimization problem. Except for a few heuristic methods, most algorithms are based on maximizing a likelihood function. In [1], for the NDA symbol timing recovery, this criterion yields the objective function $\Lambda(\tau)$, which is equal to

$$\Lambda(\tau) = \sum_{i=1}^{N} |x_i(\tau)|^2, \tag{2}$$

while the DA carrier frequency recovery often uses the objective function $\Lambda(\tau)$, defined as

$$\Lambda(f_\Delta) = \left| \sum_{i=1}^{N} c_i^* x_i(\tau, f_\Delta) \right|, \tag{3}$$

where c_i^* is the complex conjugate of the i-th training symbol. These two objective functions are actually aimed at maximizing the energy of the data sample set. This ML based estimation method uses second-order statistics of the samples and is suitable for linear channels with additive white Gaussian noise (AWGN). However, for channels that are dominated by ISI, and cannot be modeled with second-order statistics appropriately [11], a criterion that considers higher order statistics is a more reasonable approximation.

The entropy is a measure of randomness or uncertainty of a signal, and it is a function of the signal PDF. As explained in [12], the higher order statistics are taken into consideration by measuring entropy. According to information theory, the minimum entropy of any type of communication signal is equal to the entropy of the transmitted information. It is understood that the purpose of synchronization is to remove the interference due to the STO and CFO. This specific interference introduces extra entropy to the received signal and,

as such, the entropy can be used as a cost function towards synchronization. Unlike the ML criterion, the EM criterion does not model the interference using a statistical model, making it difficult to prove the EM criterion mathematically. However, it will be demonstrated through rigorous numerical simulations in the rest of the paper.

The Shannon entropy is the most commonly used measure of the quantity of information embedded in a signal. Assuming M possible observations of a one-dimensional discrete signal, with p_k representing the probability of the k-th occurrence, the Shannon information entropy H_S is expressed as [13]

$$H_S = -\sum_{k=1}^{M} p_k \log p_k, \tag{4}$$

where the logarithmic function usually uses base two, and the corresponding entropy unit is expressed in *bits*. In the next two sections, the Shannon entropy is used as a metric to evaluate the eye diagram and constellation diagram.

C. EYE DIAGRAM ENTROPY AND SYMBOL TIMING RECOVERY

To recover the symbol timing, in this work the entropy of the eye diagram is utilized. Ideally, the down-sampling instant should be located in the middle of the eye diagram where the eye opening reaches its maximum. The symbol timing recovery can be then interpreted as an algorithm to adjust the timing instant with a proper STO on the eye diagram.

The eye diagram is composed of time domain signal traces that are periodically overlaid in a window with a length of one or two symbol periods. The *eye diagram entropy* is defined as the entropy of the signal that is distributed at a certain timing instant on the eye diagram. This can be further explained using Fig. 1. The eye diagram in Fig. 1(a) is sliced vertically at four timing instants. The signal probability distributions at each timing instant are estimated using the histogram in Fig. 1(b). The histogram is a simple visualization of the data distribution where bins are defined, and the number of data samples within each bin is tallied. Here the number of samples is normalized and presented as probabilities. Then, the eye diagram entropy can be found using (4).

For example, a given modulation scheme with an alphabet size of M is implemented to transmit random data in an ideal channel. At the receiver, with perfect timing recovery, the signal samples can only be distributed equally within M possible symbols. The probability that the samples belong to the k-th symbol is $p_k = 1/M$. Substituting p_k into (4), the minimum eye diagram entropy is defined as

$$\min H_{eye} = -\sum_{k=1}^{M} \frac{1}{M} \log_2 \frac{1}{M} = \log_2 M, \tag{5}$$

which is exactly the same as the amount of information carried by each symbol.

The minimum eye diagram entropy only exists when the perfect symbol timing is achieved, because according to the
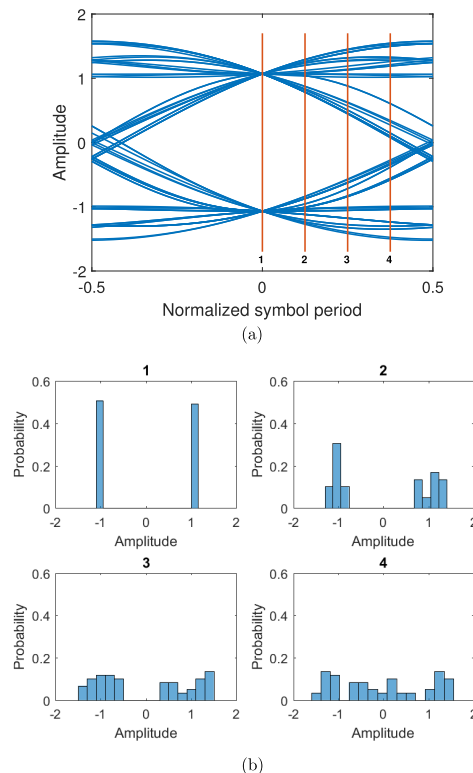

FIGURE 1. Signal probability distribution at four timing instants on a typical eye diagram. (a) Timing instants on a typical eyediagram. (b) Histograms of signal probability distribution.

Nyquist criterion, there is zero ISI at these timing instants. For a timing instant that deviates from the middle of the eye, the Nyquist criterion is violated and the interference from adjacent symbols increases the randomness. An analytical relationship between the eye diagram entropy and the timing instant is difficult to demonstrate; however, it can be observed that as the timing instant shifts away from the center, the signal energy from current symbol decays, and the interference energy grows, leading to increased randomness. Therefore, the entropy, being a measure of randomness, will also increase. Since each interference pulse from adjacent symbols carries the same amount of information, if the span of the pulse shaping filter is N_{span}, the maximum eye diagram entropy will be N_{span} times the amount of information carried by each symbol, which can be presented as

$$\max H_{eye} = N_{span} \log_2 M. \tag{6}$$

To summarize, the EM based symbol timing recovery seeks the timing instant with minimum eye diagram entropy. The eye diagram entropy can be seen as an indicator of the ISI that is introduced by adjacent symbols. Effectively, the desired timing instant with zero ISI is the instant with minimum eye diagram entropy.

D. CONSTELLATION DIAGRAM ENTROPY AND CARRIER FREQUENCY RECOVERY

The EM criterion can also be applied to recover the carrier frequency. When the passband signal is down converted to

baseband, the complex data can be visualized as a constellation diagram. However, if the frequency of the local oscillator is different (even by a very small margin) from the carrier of the signal, the resulting constellation diagram rotates and cannot be demodulated reliably. The estimation of a CFO that is much smaller than the symbol rate is discussed in this section, since for a large CFO, a preceding coarse carrier recovery is usually required.
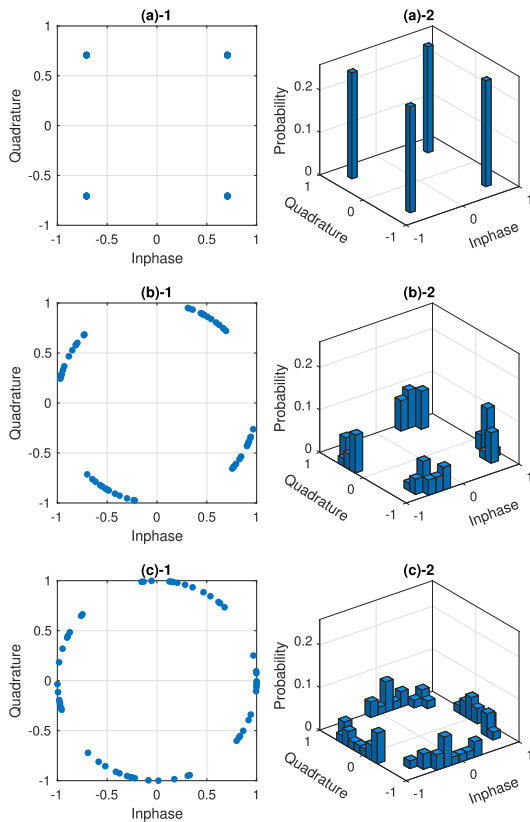

FIGURE 2. Constellation diagrams with different CFOs and the corresponding histograms of signal probability distribution.

The randomness of the signal distribution on the constellation diagram can be quantitatively measured by the *constellation diagram entropy*. Similar to the eye diagram entropy, the histogram can be used for probability estimation. However, a 2D histogram is needed to present both in-phase and quadrature components (or phase and amplitude components when considering the polar coordinate system) on the constellation diagram. Examples of noise free QPSK constellation diagrams with zero, mild and strong CFO with their corresponding histograms are shown in Fig. 2. The constellation diagram entropy can be estimated with these 2D histograms. According to (4), the highest probability peaks in the histogram indicate the lowest entropy (as observed in Fig. 2(a)). The probability that a sample occupies a given bin can be roughly considered to be equal in all bins. Therefore, it can be approximated by $p_{const} \approx 1/n_{bin}$, where n_{bin} is the number of histogram bins loaded with signal samples.

Thus, the constellation entropy is given by

$$H_{const} \approx -n_{bin}p_{const}\log_2 p_{const} \approx -\log_2\frac{1}{n_{bin}}. \quad (7)$$

For example, when the CFO is zero, $\min n_{bin} = M$, and the minimum constellation entropy is

$$\min H_{const} = \log_2 M, \quad (8)$$

which is the same as (5). There is also an upper limit on the constellation entropy when the rotation of the constellation results in samples that are uniformly distributed along a circle such that separate clusters can no longer be distinguished. This phenomenon will be further discussed in Section III-C. Note that an analytical discussion is provided in [8] and demonstrates that, for PSK modulation, the entropy has a global minimum and corresponds to a CFO equal to zero.

III. IMPLEMENTATION OF SYMBOL TIMING AND CARRIER FREQUENCY ESTIMATION

In this section, a customized entropy estimation algorithm is provided. Then the EM criterion will be implemented for symbol timing and carrier frequency estimation. Practical issues are addressed, and the estimation algorithms are discussed in detail.

A. CUSTOMIZED ENTROPY ESTIMATION ALGORITHM

According to the Shannon entropy defined by (4), the entropy is a function of the PDF of the observations. A common technique is to use the histogram for probability estimation as shown in Fig. 1 and Fig. 2. In this section, the Rényi entropy is utilized as an alternative customized entropy estimation algorithm for the purpose of conceptual verification.

The Rényi entropy is a generalization of the Shannon entropy. It is defined as [14]

$$H_R = \frac{1}{1-\beta}\log\left(\sum_{k=1}^{M}p_k^{\beta}\right), \quad (9)$$

where β is the order of the Rényi entropy. As explained in [15], when the order $\beta \rightarrow 1$, the Rényi entropy tends to be equal to the Shannon entropy. Following [12] the quadratic Rényi entropy ($\beta = 2$) is chosen in this work such that a further simplification can be made. Using $\beta = 2$ in (9), the quadratic Rényi entropy is given by

$$H_{R2} = -\log\left(\sum_{k=1}^{M}p_k^2\right). \quad (10)$$

Note that in (10), the logarithm function is external to the sum of the quadratic probabilities. Because the logarithm function is monotonic, minimizing (10) is equivalent to maximizing its internal portion. Since the search for a minimum entropy relies on a relative value of H_{R2}, the logarithm function can be dropped out without affecting the estimation result. This can be attractive when implemented on elementary processors that cannot process advanced math functions. Recall that for

the Shannon entropy given in (4), the sum of $p_k \log p_k$ is simplified to the sum of p_k^2 here.

As suggested in [16], the kernel density estimation (KDE) is used to evaluate the argument of the logarithm function in (10). As such, for a set of N samples, $i = 1, \ldots, N$, the sample probability at an observation ξ can be estimated by

$$p(\xi) = \frac{1}{N} \sum_{i=1}^{N} K_r (\xi - x_i), \qquad (11)$$

where $K_r(\cdot)$ is a kernel function with a positive parameter r. Then, by substituting (11) into (10) and after some simplification, we have

$$H_{R2} = -\log \left(\frac{1}{N^2} \sum_{i=1}^{N} \sum_{j=1}^{N} K_r (x_i - x_j) \right), \qquad (12)$$

where p_k^2 in (10) is directly estimated by the kernel function. The simplest kernel function, the top-hat kernel is given by

$$K_r(x) = \begin{cases} 1, & |x| \leq r \\ 0, & \text{otherwise.} \end{cases} \qquad (13)$$

where the threshold r is used to determine the quantization level in which samples are grouped for entropy estimation. The choice of r will be detailed later in this section. Using (12) and (13), the entropy can be estimated by measuring the distances between samples instead of using histograms.

From the discussion above, the customized entropy estimation algorithm is summarized using the following steps:

1) For a given set of observations with N samples, calculate all the distances d_{ij} between each sample pair x_i and x_j, where $1 \leq i < N$ and $i < j \leq N$. Then, the distance d_{ij} is given by

$$d_{ij} = \| x_i - x_j \|, \qquad (14)$$

where $\|\cdot\|$ represents the Euclidean norm.
2) Define a separation threshold r and count the number of d_{ij} that satisfy $d_{ij} > r$, and denote the number of separated sample pairs as H_{sp}.
3) After normalization, express the modified Rényi entropy (MRE) as

$$H_{MRE} = \frac{H_{sp}}{N(N-1)/2}. \qquad (15)$$

The resulting H_{MRE} is the modified version of the quadratic Rényi entropy in which the logarithm function is dropped. Because of the normalization, the value of H_{MRE} is limited between 0 to 1 and is unitless. Intuitively, H_{MRE} is a measure of the amount of sample dispersion, since it counts the number of sample pairs with distances greater than the threshold r.

The choice of the threshold r (often referred as bandwidth in KDE [17]) exhibits a strong influence on the results. It can be derived arithmetically from sophisticated algorithms to achieve an optimal probability estimate [17]. Note that the absolute entropy value is not important, and the threshold r

is empirically set to be equal to the root-mean-square value of the noise.

Another design parameter for MRE estimation is the number of samples, which is equal to a few hundred in our application. Entropy estimation is more accurate with a growing number of samples, but the number of distance calculations grows quadratically. Note that the computational complexity can be reduced by using other distance metrics presented in [18]. However, this will cause a reduced tracking ability, which means that the algorithm cannot adapt to the time varying channel effectively. As such, the choice for the number of samples depends both on the dynamic channel conditions and the hardware capabilities.

B. SYMBOL TIMING OFFSET ESTIMATION

STO estimation can be implemented by searching for the instant with minimum entropy in the eye diagram. In this section, the following practical issues are addressed: 1) resolving local minima in the entropy curve, 2) examining the timing recovery in presence of CFO, and 3) providing accurate STO estimation at low oversampling rate.

The entropy reaches a global minimum in the center of the eye diagram, but in practice, when the timing instant is close to the symbol transition area, the entropy may decrease and create local minima. Local minima could result in false STO estimation especially at low SNR conditions, and particularly if gradient based search algorithms are used. Since the entropy local minima occur when the sample magnitude is small, an additional threshold can be introduced to eliminate these data samples in the entropy estimation.

The following steps summarize the MRE estimation algorithm with the additional threshold:

1) Define a threshold r_{mg} and build a new sample set where all samples with a magnitude greater than r_{mg} are included. The number of samples in the new set is denoted as N_{mg};
2) Find all the Euclidean distances d_{ij} between each sample pair x_i and x_j in the new sample set, where $1 \leq i < N_{mg}$ and $i < j \leq N_{mg}$;
3) Define an aggregation threshold r. Count the number of d_{ij} for which $d_{ij} < r$ (note this inequality is different from its counterpart in Section III-A), and denote the number of aggregated sample pairs as H_{ag};
4) Express the bounded modified Rényi entropy (BMRE) as

$$H_{BMRE} = 1 - \frac{H_{ag}}{N(N-1)/2}. \qquad (16)$$

A typical case is given here to show how the EM based STO estimation works. The received signal consists of a frame of QPSK modulated random symbols, which are pulse shaped to generate a baseband complex envelope. The oversampling rate is 40 to provide a better eye diagram resolution. An AWGN channel is assumed with $E_s/N_0 = 18$ dB. After the matched filter, the eye diagram of the real component of the signal is shown in the upper part of Fig. 3, and both the

MRE and BMRE estimation results are shown in the lower part. The thresholds are $r = 0.25$ and $r_{mg} = 0.3$.
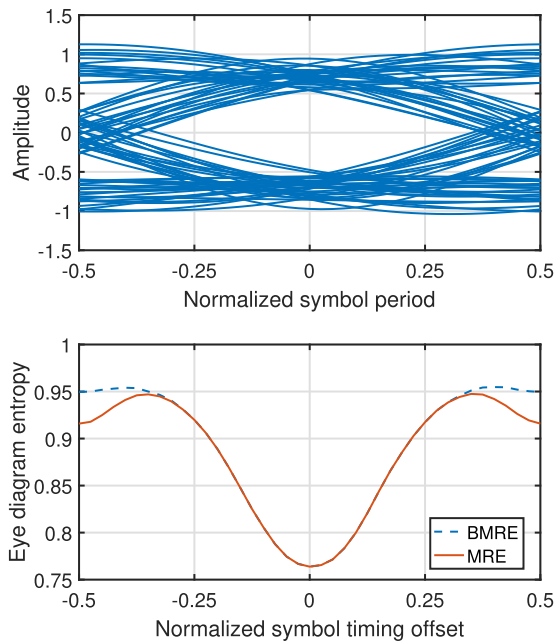

FIGURE 3. An typical eye diagram (upper) and the corresponding eye diagram entropy (lower).

In Fig. 3, the entropy reaches a global minimum in the center of the eye diagram, and its value is close to 0.75. This minimum entropy value can be derived as follows. Since the QPSK symbols are i.i.d, there are four clusters distributed on the constellation diagram, and each cluster consists of $N/4$ samples. The threshold r is designed such that the condition of $d_{ij} < r$ can only be satisfied between samples located in the same cluster. For 4 clusters, $H_{ag} \approx 4(N/4)^2/2$ (assuming $N \gg 1$). Thus, the minimum value of the BMRE is approximated by

$$\min H_{BMRE} \approx 1 - \frac{4(N/4)^2/2}{N^2/2} = 0.75. \qquad (17)$$

The minimum value of MRE in the eye diagram center can also be derived in a similar way to the BMRE. The entropy increases with the absolute value of STO, indicating more randomness introduced by ISI. When the STO is beyond ± 0.35, the MRE estimation decreases and creates a local minimum in the symbol transition. This phenomenon is also illustrated in the eye diagram, where the samples aggregate into three visible groups (with amplitudes of ± 1 and 0).

The result of the BMRE algorithm coincides with that of the original MRE algorithm in most of the timing instants, but the local minima near ± 0.5 become flat. As such, with the BMRE estimation algorithm, the local entropy minima due to the symbol transitions are removed, and the STO can be estimated with higher accuracy.

Next, the impact of timing recovery in presence of uncompensated CFO will be evaluated. Theoretically, the previous analysis of eye diagram entropy still holds, but the CFO does introduce extra entropy in the estimation. To understand how the CFO affects the eye diagram entropy, another simulation that is similar to what was demonstrated in the early part of this section is conducted with an extra CFO at 1% of the symbol rate introduced. The eye diagram and the corresponding entropy are depicted in Fig. 4.
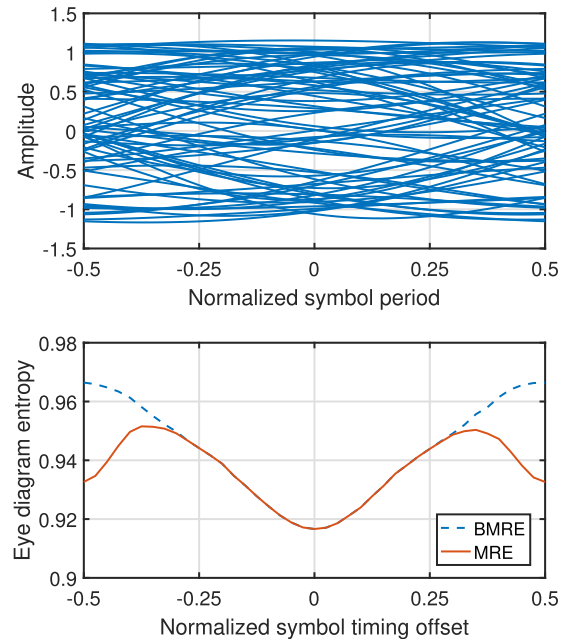

FIGURE 4. An eye diagram with carrier frequency offset (upper) and the corresponding eye diagram entropy (lower).

The eye diagram shows an eye that is completely closed: the center of the eye or optimum timing instant cannot be identified by only observing the eye diagram. However, the optimum timing instant can be clearly identified with the entropy curve. Both the MRE and the BMRE algorithms have the same global minimum at zero STO.

In Fig. 4, it is also interesting to observe the entropy plot at a symbol transition. With the MRE algorithm, the local minima are more noticeable and may lead to a false STO estimate. However, the BMRE algorithm shows superior performance: the curve is not flat anymore but continues growing with the same gradient as a function of timing offset. This feature shows a good adaptation of the BMRE algorithm and proves that the "symbol timing recovery before carrier recovery" receiver configuration is feasible.

In the previous discussion, a global search for STO with minimum eye diagram entropy requires a high oversampling rate (normally more than 10 samples per symbol). However, this is not always available in practice, especially for high speed communication. Recall that the O&M algorithm uses as low as 4 samples per symbol, and its STO is given by

$$\tau = \frac{T}{2\pi} \arg \left\{ \sum_{i=1}^{N} |x_i|^2 e^{-j2\pi(i-1)/N_{sps}} \right\}, \qquad (18)$$

where T is the symbol period and N_{sps} is the oversampling rate. The operation $\arg\{\cdot\}$ returns the phase angles in radians.

The guiding principle of the O&M algorithm is to apply a discrete Fourier transform (DFT) to the squared signal x_i^2, and the STO is extracted from the angle of the resulting spectrum line at the symbol rate.

The theory behind (18) is that the squared signal x_i^2 is a periodic signal with the same frequency and phase as the pulse shaped symbols due to the cyclostationary property of x_i. Thus, even with a low oversampling rate, the STO can still be estimated by DFT. The eye diagram entropy curve exhibits a similar property as x_i^2 within one period. Therefore, the same approach can be applied to the EM based symbol timing algorithm. To be specific, x_i^2 in (18) can be replaced with the eye diagram entropy H_i, such that the STO can be found with

$$\tau = \frac{T}{2\pi} \arg \left\{ \sum_{i=1}^{N_{sps}} H_i e^{-j2\pi(i-1)/N_{sps}} \right\}. \tag{19}$$

Note that (19) assumes that the entropy curve is symmetric to the center of the eye diagram, but the symmetry may not be maintained at low SNR or in a multipath channel. In these conditions, the algorithm may result in large estimation variance.

Although the complexity of the STO estimation is reduced by using less samples (similar to the O&M algorithm), the EM based method still requires higher computational load than conventional algorithms, because of the nature of entropy estimation. The MRE and BMRE algorithms can relieve certain computational load by using approximation methods, but the complexity remains higher than the conventional methods. Nonetheless, the entropy analysis provides more insights on the signal eye diagram and helps locate the maximum eye opening, as will be shown in Section IV.

The STO estimation discussed in this section assumes that the symbol period is known to the receiver and that there is no time scaling during transmission. Thus, the symbol timing recovery discussed here is equivalent to locating a timing offset on the eye diagram. If this assumption does not hold, a symbol period estimation is required. Such an estimation can be done by searching for the symbol period that can minimize the whole eye diagram entropy.

C. CARRIER FREQUENCY ESTIMATION

In this section, the implementation of the EM based CFO estimation algorithm is detailed. Similarly to the STO estimation discussed above, the proposed algorithm is also NDA. The constellation diagram entropy is measured by defining an adequate range for the trial CFO, and a global search is applied to find the minimum entropy. The characteristics of the entropy curve are shown first and then a method that can increase the global search efficiency is proposed.

In Section II-D, it can be noted that the constellation entropy is almost flat when the CFO is greater than a maximum frequency. This maximum frequency can be considered as the effective search range for EM based CFO estimation. The entropy curve within the frequency limit has a V-shape

"trough" (negative peak) and the entropy global minimum is located in the middle of the trough. For a given modulation scheme, the range of the trough is affected by the CFO (f_Δ), the symbol rate $1/T$, and the number of data samples N in the window. For example, the M-PSK modulated signal has a minimum constellation phase difference $2\pi/M$. The accumulated phase shift due to CFO is given by $2\pi f_\Delta NT$. The constellation entropy increases with the CFO until the accumulated phase shift is greater than the minimum constellation phase difference. Therefore, the CFO search range is given by

$$|f_\Delta| < \frac{1}{MNT}, \tag{20}$$

and when the CFO is larger than $1/MNT$, the entropy curve becomes flat.

Using (20), if N is equal to a few hundred samples, a given CFO that can fall into the entropy search range must be on the order of 0.1% of the symbol rate, which is relatively small compared to the CFO range that needs to be covered. The resulting entropy curve as a function of trial CFO is generally flat with the exception of a sharp trough. A similar result has also been reported in [8]. Consequently, the linear search requires very fine steps to achieve high frequency resolution, and the potential gradient descent algorithm may not converge due to lack of gradient. In other words, an efficient search algorithm cannot be applied.

In order to cover a large estimation range without intensive computation, an algorithm that can expand the width of the trough is required. To increase the trough width, a possible solution is to reduce N. However, the lack of samples will lead to an inaccurate PDF and entropy estimation. Instead, a block average algorithm inspired by [19] is adopted to smooth the entropy curve. The data samples are equally segmented into L blocks, and the entropy of the i-th block is denoted as $H_i(f_\Delta)$. The block averaged constellation diagram entropy is given by

$$H_{const}(f_\Delta) = \frac{1}{L} \sum_{i=1}^{L} H_i(f_\Delta). \tag{21}$$

The CFO is assumed to be constant for the set of data samples. Thus, each block possesses the same entropy curve but with random fluctuation due to the lack of samples for probability estimation. By averaging the entropy curve using small blocks, a wide and smooth entropy trough is achieved. The new trough is L times wider than the original one.

With the same settings as in Section III-B, the numerical simulation of the constellation diagram entropy is compared using 1) 400 samples, 2) 50 samples and 3) block averaged 400 samples with a block size of 50 samples ($L = 8$). The results are plotted as a function of the CFO in Fig. 5. Perfect symbol timing is assumed, and the CFO search range is swept within 1% of the symbol rate.

As discussed in Section II-D, the entropy curve should reach the global minimum with the CFO equal to zero. In Fig. 5, the entropy curve using 400 samples has only one global minimum when the CFO is equal to zero and no other local minimum. But its curve has a very narrow
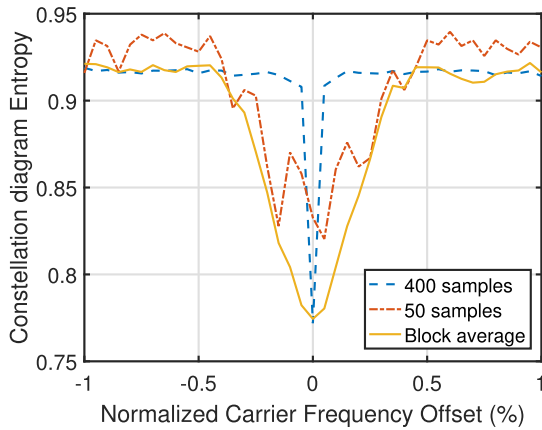
FIGURE 5. Constellation diagram entropy for carrier frequency recovery.

trough as predicted. The entropy estimated using 50 samples has a trough boundary at ±0.5% of the symbol rate, which agrees with (20). In fact, the trough range is expanded by 8 times, but many fluctuations and local minima appear. In comparison, the entropy curve using the block averaging has the same expanded trough as the entropy estimated using 50 samples, but the local minima are smoothed out, leaving only the global minimum at the zero CFO.

Given the expanded entropy trough, a more efficient two-step linear search, similar to the algorithm described in [8], can be readily applied. First, a coarse search through the frequency range of interest with step size equal to the half trough width can provide an approximate CFO estimate. A second search with a fine frequency step near the coarse estimation result can improve the accuracy of the CFO estimate.

Recall that the computation complexity grows quadratically with the number of samples, so breaking down the sample set into small blocks can significantly reduce the required computation. For example, if the 400 samples are equally divided into 8 blocks, it is easy to find that compared to the algorithm without block averaging, this algorithm requires eight times less number of Euclidean distance calculations (defined by (14)). This is a significant reduction in computational complexity.

Compared to the linear search algorithm proposed in [8], the block average method for CFO estimation reduces the computational complexity by calculating less sample pair distances. However, similar to the STO estimation using (19), it is still more complex than the conventional ML based algorithms because of the estimation of entropy instead of energy. The EM based algorithms are not appropriate for computation sensitive tasks. On the other hand, note that since the computing of the entropy for each trial STO or CFO is independent, it is possible to perform in parallel mode (such as using a multi-core processor or FPGA) to accelerate the estimation.

IV. PERFORMANCE EVALUATION

In this section, the performance of the symbol timing and carrier frequency estimation algorithms presented in the

previous section are assessed in controlled conditions. The estimation error variance in AWGN channel is used as the major figure of merit. Also, the effect of multipath impairment is analyzed on the system performance.

First, the performance of the symbol timing estimation algorithm (19) is examined in presence of AWGN. The O&M algorithm described by (18) is used here to represent the ML estimator for comparison.
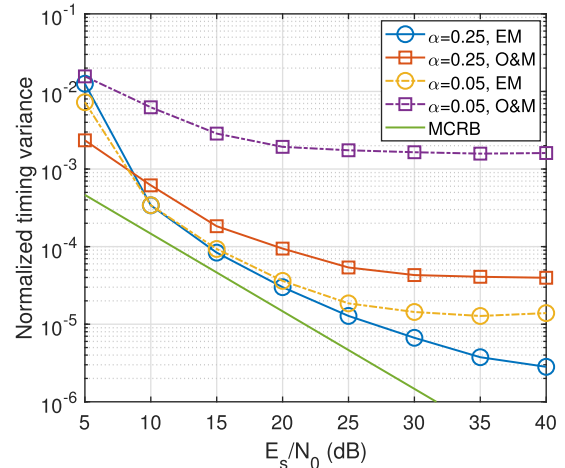

FIGURE 6. Timing error variance of two symbol timing algorithms with two rolloff factors.

The performance comparison in presence of AWGN is shown in Fig. 6. In this figure, the QPSK modulation is evaluated, but similar results are expected for other PSK or QAM modulation schemes. A pulse shaping filter is used to limit the bandwidth. The rolloff factor used in the evaluation is $\alpha = 0.25$ and 0.05 respectively. The small excess bandwidth conditions are chosen to accommodate a recent bandwidth efficient communication standard [20]. The choice is also motivated by the fact that using small rolloff factor represents the worst case with respect to the timing error variance.

AWGN is introduced at the receiver, such that the symbol energy to noise spectral density ratio (E_s/N_0) ranges from 5 to 40 dB. For each E_s/N_0 setting, the average of 500 Monte Carlo trials are taken. In each trial, a block size of 100 symbols are used to estimate the STO. The proposed algorithm (19) is used for the EM based STO estimation. After normalization by the symbol period, the variances of the timing error (also known as the jitter variance in some literature [21]) with respect to the symbol period are represented in Fig. 6. Following [1], the modified Cramér-Rao bound (MCRB) is also shown as the theoretical limit.

Several conclusions can be drawn from Fig. 6. Generally, the EM based symbol timing algorithm has lower error variance than the O&M algorithm for both rolloff factors and for a large range of E_s/N_0. With the O&M algorithm, larger rolloff factor generates smaller error variance. When the E_s/N_0 is greater than 25 dB, the variance value reaches a lower limit because of its strong self-noise [1]. In contrast, the timing error variance of the EM based algorithm changes less

significantly with different rolloff factors. Also, it suffers less from the self-noise.

The O&M algorithm has less error variance when $E_s/N_0 < 9$ dB and $\alpha = 0.25$. This is because the O&M algorithm, as an example ML algorithm, is designed under AWGN assumption. In fact, the EM based algorithm is favored in small excess bandwidth conditions, because the eye diagram entropy estimation can effectively measure the ISI. However, if a pulse shaping filter with larger excess bandwidth is used ($\alpha > 0.5$ for example), the O&M algorithm will have a performance very close to the MCRB [1].

As explained in Section III-B, the EM based symbol timing estimation is insensitive to the CFO, but it is interesting to understand how the performance changes in the presence of CFO. The simulation settings are generally the same as for the last one, except that different modulation schemes, BPSK and QPSK, are evaluated, and the rolloff factor is set to 0.25. The introduced CFO is 1% of the symbol rate, and the timing variances are plotted in Fig. 7.
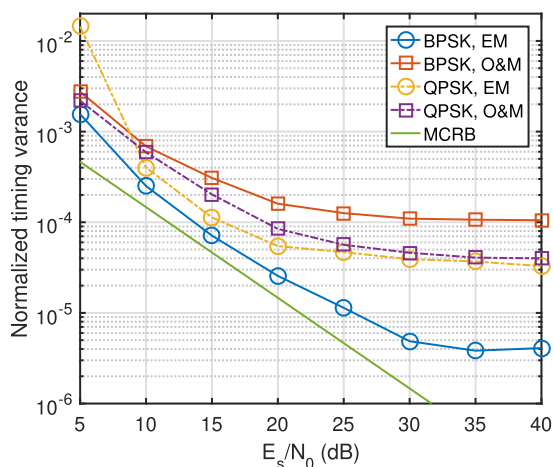

FIGURE 7. Performance of two symbol timing estimation algorithms in the presence of CFO.

For BPSK modulation, the EM based algorithm shows a good performance that is close to the MCRB when the E_s/N_0 is below 30 dB. It has the highest performance improvement compared to the O&M algorithm. However, for QPSK modulation, the performance improvement is marginal. This is because, for the EM based algorithm in (19), it is assumed that the eye diagram entropy curve is symmetrical to the center of the eye diagram, and this only stands with low modulation order and low noise level. Another example of an asymmetrical eye diagram entropy condition will be analyzed in the following simulation.

A key issue that coherent communication systems are facing is the multipath channel impairment. Unpredictable channel impulse responses violate the Nyquist ISI criterion, and the communication performance is compromised. The nature of EM based symbol timing estimation is to search for the timing instant with minimum ISI, which makes it more suitable for these conditions than ML based algorithms.

To demonstrate this, a set of BPSK modulated symbols with $\alpha = 0.5$ is transmitted. For simplicity, a multipath channel with impulse response $h(t)$ is given by

$$h(t) = \delta(t) + 0.5\delta(t - 1.4T) + 0.2\delta(t - 3.5T). \quad (22)$$

At the receiver, the eye diagram and the timing instants estimated by both O&M and EM algorithms are plotted in Fig. 8 for E_s/N_0 equal to 15 dB.
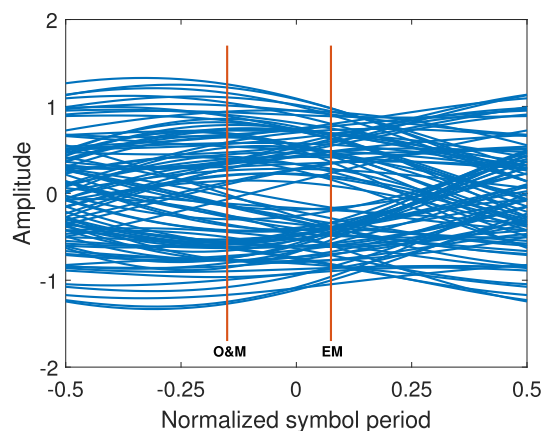

FIGURE 8. An eye diagram after a multipath channel and the corresponding timing estimation results.

The eye diagram in Fig. 8 is almost closed and shifted from the center due to ISI. The bit error rates (BER) of demodulated samples recovered by the two algorithms are compared without equalization. The EM algorithm can find the maximum eye opening and achieves a BER of 1.2%. In contrast, the BER is 5.9% if using the O&M algorithm. As one can observe in Fig. 8, the samples recovered by the O&M algorithm have the highest energy output, but with strong ISI.

The results from the channel given by (22) is not a special case. To evaluate the timing recovery algorithms in realistic multipath channel conditions, a measured impulse response of an underwater acoustic channel in Fig. 9 is considered. The multipath channel models utilize the amplitudes and delays of the five greatest impulses from the measured data. Both Rayleigh and Rician fading are tested, where the Rician K-factor is set to 3. The channel model is quasi-static, such that the channel parameters are constant within each trial. The final results are the average of 500 Monte Carlo trials.

The transmit signal are QPSK modulated, and 3000 random symbols are sent in each trial with a symbol rate of 240 Bd. At the receiver side, a symbol-spaced decision feedback equalizer is placed after the timing recovery to compensate for the multipath channel. Both the equalizer's feedforward and feedback filters have 6 complex weights. The adaptive algorithm used in the equalizer is a recursive least square (RLS) with a forgetting factor of 0.95. The first 1000 symbols are the training signal, and the symbol error rate (SER) is calculated with the equalizer's output for the rest 2000 symbols.
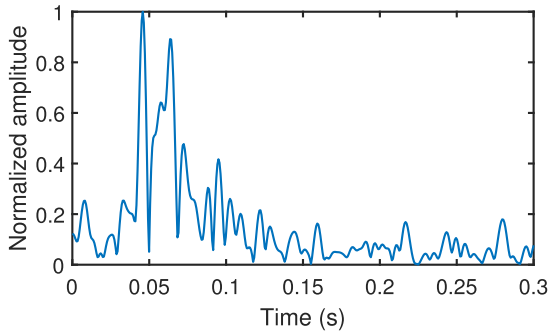
FIGURE 9. Impulse response of a multipath underwater acoustic channel.

TABLE 1. Symbol error rate (%) in multipath fading channels.

Fading	Rolloff	Mid	O&M	EM
Rayleigh	0.75	0.36	13.35	1.59
	0.5	1.10	16.02	2.67
	0.25	6.27	16.43	5.85
	0.05	20.38	26.34	14.04
Rician	0.75	0.17	11.92	1.27
	0.5	0.58	11.47	1.64
	0.25	3.64	12.57	3.59
	0.05	11.92	19.45	8.38

The simulation results are summarized in Table 1. The SER when synchronizing to the middle of the first arrival is also calculated as a reference. Note that if the equalizer converges during the training, the SER of a single trial is negligible. However, if it fails to converge, the SER can be up to around 75% for QPSK modulation. Therefore, the averaged SER listed in the table is an indicator of how often the equalizer fails to converge with the given timing recovered samples.

As can be observed, the SER of the EM algorithm significantly outperforms that of the O&M algorithm for all rolloff factor settings and fading conditions. As such, the equalizer is much more likely to converge using the EM based timing recovery algorithm. It can be observed in Table 1 that in small rolloff factor conditions, using the first arrival does not always provide optimum down-sampling positions, since the maximum eye opening is shifted due to ISI as shown in Fig. 8. In fact, it is clear that the EM algorithm provides better SER when the rolloff factor is small.

Next, the performance of CFO estimation in presence of AWGN is evaluated. For the carrier frequency recovery test, perfect symbol timing is assumed. The signal is QPSK modulated with a CFO equal to 1% of the symbol rate. Three algorithms are compared for CFO estimation: the EM based algorithm, the open loop and the classic ML algorithm.

The open loop algorithm proposed in [22] estimates the CFO by averaging the differential phase error over the window. For QPSK modulation, the CFO is given by [1]

$$f_\Delta = \frac{1}{8\pi T} \arg \left\{ \sum_{i=2}^{N} \left(x_i x_{i-1}^* \right)^4 \right\}. \quad (23)$$

The classic ML algorithm uses the same global search method as the EM algorithm. The objective function is

given by

$$\Lambda(f_\Delta) = \left| \sum_{i=1}^{N} x_i^4 e^{-j8\pi f_\Delta iT} \right|^2. \quad (24)$$

In (24), the CFO is estimated by searching for the trial CFO that yields the highest energy or alternatively by applying a computationally efficient FFT based implementation [6]. Note that both (23) and (24) are NDA algorithms and a power of 4 is applied to the signal to remove the modulation. This is not necessary in the EM algorithm. The CFO that is estimated using the three algorithms is normalized by the symbol rate, and for each E_s/N_0 condition, 500 trials are conducted to compute the variance. The results are shown in Fig. 10, where the MCRB is also included as a reference.
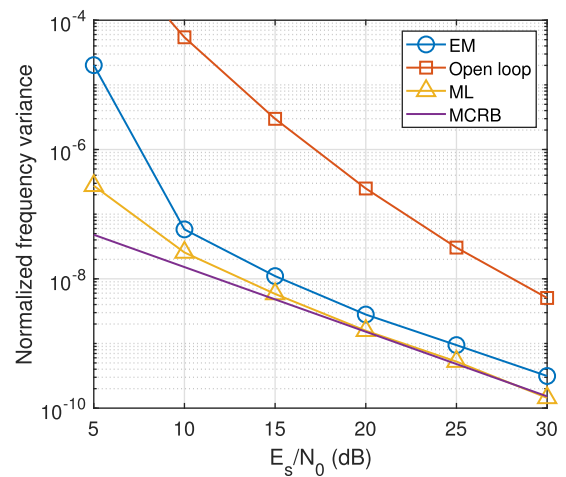

FIGURE 10. Performance of three carrier frequency recovery algorithms.

In Fig. 10, the EM algorithm shows a much smaller frequency variance than the open loop algorithm. This demonstrates its robustness for CFO estimation. However, the performance of the classic ML algorithm is mostly the same as the MCRB, making it slightly better than the EM algorithm. It is not surprising that the classic ML algorithm provides a smaller variance than the EM algorithm in AWGN, since theoretically it is the optimum solution in these conditions.

The CFO estimation performance for both the EM and classic ML algorithms in multipath channels has also been examined. The performance of the two algorithms has no significant difference in terms of SER if the same timing recovery is given. This is because no ISI gain can be provided to the EM based algorithm in contrast to its gain for the STO estimation. The EM algorithm has an estimation variance that is slightly larger than that of the classic ML algorithm, similar to the results observed in AWGN channel. Nonetheless, this demonstrates the usefulness of the proposed estimator as a universal timing recovery algorithm.

V. CONCLUSION
In this paper, entropy minimization has been proposed as a synchronization criterion for wireless coherent receivers. It is an alternative to the maximum likelihood criterion, which is

the foundation of most standard synchronization algorithms. The symbol timing and carrier frequency offset estimation are implemented by measuring the entropy of the eye diagram and the constellation diagram. The optimum timing delay is found by searching the timing instant with minimum eye diagram entropy, while the carrier frequency offset is estimated by searching through a range of frequencies to minimize the constellation diagram entropy.

Implementation constraints have also been presented. A modified version of the quadratic Rényi entropy and the kernel density estimation method are employed to estimate the probabilities. The proposed method is insensitive to the local minima and the carrier frequency offset. Also, it can extract the timing delay without the need for a high over-sampling rate. The carrier frequency recovery algorithm uses block averaging to expand the estimation range without compromising its accuracy.

Although the estimation requires more computational load than the conventional algorithms, it can provide more insights on the signal presentations. The performance of the proposed timing and frequency recovery algorithms is compared with that of standard approaches by running a set of numerical simulations. It is shown that the entropy minimization has great potential and offers certain advantages for synchronization. Particularly, in multipath fading and small excess bandwidth conditions, the timing recovery using the entropy minimization based algorithm can significantly improve the equalizer's convergence, and its symbol error rate outperforms that of the maximum likelihood based algorithm, by at least a factor of two.

REFERENCES

[1] U. Mengali and A. N. D'Andrea, *Synchronization Techniques for Digital Receivers* (Applications of Communications Theory). New York, NY, USA: Springer, 1997.

[2] M. Oerder and H. Meyr, "Digital filter and square timing recovery," *IEEE Trans. Commun.*, vol. COM-36, no. 5, pp. 605–612, May 1988. [Online]. Available: http://ieeexplore.ieee.org/document/1476/

[3] T.-K. Kim and M. Min, "Improved non-data-aided feedforward symbol timing estimator for low-rate sampling systems," *IEEE Commun. Lett.*, vol. 22, no. 5, pp. 1010–1013, May 2018.

[4] Y. Wang, E. Serpedin, and P. Ciblat, "Unified performance analysis of blind feedforward timing estimation," in *Proc. Conf. Rec. 26th Asilomar Conf. Signals, Syst. Comput.*, Pacific Grove, CA, USA, Nov. 2002, pp. 639–643.

[5] J. A. Lopez-Salcedo and G. Vazquez, "Asymptotic equivalence between the unconditional maximum likelihood and the square-law nonlinearity symbol timing estimation," *IEEE Trans. Signal Process.*, vol. 54, no. 1, pp. 244–257, Jan. 2006.

[6] Y. Wang, K. Shi, and E. Serpedin, "Non-data-aided feedforward carrier frequency offset estimators for QAM constellations: A nonlinear least-squares approach," *EURASIP J. Appl. Signal Process.*, vol. 2004, no. 13, pp. 1993–2001, Oct. 2004. [Online]. Available: https://link.springer.com/article/10.1155/S1110865704403175

[7] B. Chen, L. Xing, B. Xu, H. Zhao, and J. C. Principe, "Insights into the robustness of minimum error entropy estimation," *IEEE Trans. Neural Netw. Learn. Syst.*, vol. 29, no. 3, pp. 731–737, Mar. 2018.

[8] M. Pedzisz and A. Coatanhay, "Minimum entropy approach for carrier frequency recovery," *IEEE Trans. Wireless Commun.*, vol. 5, no. 4, pp. 774–778, Apr. 2006.

[9] X. Liu and J.-F. Bousquet, "Entropy minimization based synchronization algorithm for underwater acoustic receivers," in *Proc. Int. Conf. Underwater Netw. Syst. (WUWNET)*. New York, NY, USA: ACM, 2017, pp. 20:1–20:5. [Online]. Available: http://doi.acm.org/10.1145/3148675.3148719

[10] B. Xie, W. Qiu, and H. Minn, "Exact signal model and new carrier frequency offset compensation scheme for OFDM," *IEEE Trans. Wireless Commun.*, vol. 11, no. 2, pp. 550–555, Feb. 2012.

[11] O. Golani *et al.*, "Experimental characterization of nonlinear interference noise as a process of intersymbol interference," *Opt. Lett.*, vol. 43, no. 5, pp. 1123–1126, Mar. 2018.

[12] I. Santamaría, D. Erdogmus, and J. C. Principe, "Entropy minimization for supervised digital communications channel equalization," *IEEE Trans. Signal Process.*, vol. 50, no. 5, pp. 1184–1192, May 2002.

[13] C. E. Shannon, "A mathematical theory of communication," *Bell Syst. Tech. J.*, vol. 27, no. 3, pp. 379–423, Jul./Oct. 1948.

[14] A. Rényi, "On measures of entropy and information," in *Proc. 4th Berkeley Symp. Math. Statist. Probab.*, vol. 1, 1961, pp. 547–561.

[15] P. A. Bromiley, "Shannon entropy, Renyi entropy, and information," Memo Tech. Rep. 2004-004, 2004. [Online]. Available: https://www.researchgate.net/publication/253537416_Shannon_Entropy_Renyi_Entropy_and_Information

[16] J. C. Principe, D. Xu, Q. Zhao, and J. W. Fisher, III, "Learning from examples with information theoretic criteria," *J. VLSI Signal Process.*, vol. 26, nos. 1–2, pp. 61–77, 2000. [Online]. Available: http://link.springer.com/10.1023/A:1008143417156

[17] Z. I. Botev, J. F. Grotowski, and D. P. Kroese, "Kernel density estimation via diffusion," *Ann. Statist.*, vol. 38, no. 5, pp. 2916–2957, Oct. 2010. [Online]. Available: http://projecteuclid.org/euclid.aos/1281964340

[18] S.-H. Cha, "Comprehensive survey on distance/similarity measures between probability density functions," *Int. J. Math. Models Methods Appl. Sci.*, vol. 1, no. 4, pp. 300–307, 2007. [Online]. Available: http://citeseerx.ist.psu.edu/viewdoc/download?doi=10.1.1.154.8446&rep=rep1&type=pdf

[19] Y. Huang and Y. Lu, "Small carrier frequency difference detection based on the relative phase entropy," in *Proc. Int. Symp. Commun. Inf. Technol. (ISCIT)*, Oct. 2007, pp. 1417–1422.

[20] A. Morello and V. Mignone, "DVB-S2X: The new extensions to the second generation DVB satellite standard DVB-S2," *Int. J. Satell. Commun. Netw.*, vol. 34, no. 3, pp. 323–325, May 2016, doi: 10.1002/sat.1167.

[21] W. Gappmair, S. Cioni, G. E. Corazza, and O. Koudelka, "Jitter floor elimination for blind feedforward/feedback symbol-timing recovery exploiting the extended zero-crossing property," *Int. J. Satell. Commun. Netw.*, vol. 34, no. 5, pp. 645–660, Sep. 2016. [Online]. Available: http://doi.wiley.com/10.1002/sat.1162

[22] J. C.-I. Chuang and N. R. Sollenberger, "Burst coherent demodulation with combined symbol timing, frequency offset estimation, and diversity selection," *IEEE Trans. Commun.*, vol. 39, no. 7, pp. 1157–1164, Jul. 1991.
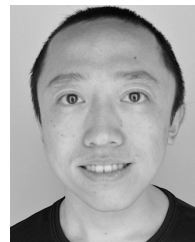
XIAO LIU received the bachelor's degree in electronic and information engineering and the master's degree in signal and information processing from the College of Underwater Acoustic Engineering, Harbin Engineering University, China, in 2008 and 2011, respectively. He is currently pursuing the Ph.D. degree with the Electrical and Computer Engineering Department, Dalhousie University. He is under the supervision of Dr. J.-F. Bousquet at the UW-STREAM Lab. His current research interests include synchronization techniques and deep learning applications for coherent wireless receivers and its implementation.

JEAN-FRANÇOIS BOUSQUET received the B.Eng. degree in electrical engineering from the École Polytechnique de Montréal in 2001 and the M.Sc. and Ph.D. degrees in electrical engineering from the University of Calgary in 2007 and 2011, respectively, with a focus on the implementation of low-power integrated circuits applied to wireless communication. From 2009 to 2011, he was a High-Speed Analog IC Designer, Ciena, where he was involved in the development of coherent fiber optics communication networks. He joined the Electrical and Computer Engineering Department, Dalhousie University, in 2013. His research interests include analog and mixed-signal integrated circuit design, digital communications, and channel characterization and estimation applied to underwater communications.

● ● ●